3D MHD Free Surface Fluid Flow Simulation Based on Magnetic-Field Induction Equations

H.L. HUANG, A. YING, M. A. ABDOU

Mechanical and Aerospace Engineering Department, UCLA, Los Angeles, CA, 90095

Huang@fusion.ucla.edu

Abstract: The purpose of this paper is to present our recent efforts on 3D MHD model development and our results based on the technique derived from induced-magnetic-field equations. Two important features are utilized in our numerical method to obtain convergent solutions. First, a penalty factor is introduced in order to force the local divergence free condition of the magnetic fields. The second is that we extend the insulating wall thickness to ensure that the induced magnetic field at its boundaries is null. These simulation results for lithium film free surface flows under NSTX outboard mid-plane magnetic field configurations have shown that 3D MHD effects from a surface normal field gradient cause return currents to interact with surface normal fields and produce unfavorable MHD forces. This leads to a substantial change in flow pattern and a reduction in flow velocity, with most of the flow spilling over one side of the chute. These critical phenomena can not be revealed by 2D models. Additionally, a design which overcomes these undesired flow characteristics is obtained.

0. Introduction

To fully understand how liquid metal MHD flows in a fusion device, 3-D numerical simulation has to be applied. Despite rapid advancements in computer resources and numerical

methods over the two last decades, magnetohydrodynamic (MHD) research remains primarily analytical/experimental in nature. Although the absolute number of numerical articles on MHD has been constantly increasing, most approaches are still formulated in one or two dimensions. Importantly, without using 3D formulations, numerical solutions can not capture the essential essence of the problems, and often provide providing poor information[1]. Furthermore, numerical codes based on the approach of solving the electrical potential equation[2] can only be applied to relatively weak magnetic fields (a few orders of magnitude weaker than those required for fusion plasma confinement). They also encounter considerable convergent difficulty if the Hartmann number becomes high (e. g. ~300). For a closed channel, a widely used method for MHD flow calculations in strong magnetic fields is the core flow approximation. The core flow approach divides a calculational domain into the core and boundary regimes, and gives the core solutions by neglecting induced magnetic fields, inertia effects, and viscous effects. The core flow approach fails when the conductivity of the channel wall becomes comparable to that of the viscous boundary layer or insulating wall[3]. Consequently, it cannot be used in a case where a free varied surface is involved because the detailed flow structures in the viscous layer and free surface have to be taken into account in order to provide a closed current path. The numerical simulation becomes even more complicated with low field cases, such as seen in NSTX (see Figure 1), since the fields are not strong enough to completely suppress the turbulence, while leaving a MHD turbulent flow still to be studied.

The goal of this MHD model development is to provide design information for the APEX study in order to evaluate the feasibility of a fast free lithium surface for particle and heat removal in a near term physics device. Considering that at any given point in time the velocity field of the main hydrodynamic quantity can be directly relating with the main electromagnetic

one (the magnetic field) without any interference it is possible to build a MHD module into an existing CFD code (FLOW-3D[4] in this case), which has a verified Navier-Stoke's solver for turbulent, free surface flows. The MHD effect is reflected in an additional term of Lorentz force in the momentum equation at each time step. In the present model, the MHD Lorentz force caused by the induced current is derived from the Ampere's law by solving the induced magnetic field equations.

Results based on the induced magnetic field formulation are presented for free lithium surface flow characteristics under NSTX outboard mid-plane field configurations. In section I, the governing equations of MHD flows are described. In particular, a conservative formulation similar to Salah[5] is applied, which leads to the introduction of a penalty factor to impose the local divergence free condition of the magnetic fields. Furthermore, to ensure proper treatment of the boundary conditions, a technique of extending insulating wall thickness is derived. In section 2, the numerical strategy is presented, while the results are reported in section 3.

1. The governing equations

The flow of an electrically conducting fluid under the influence of an external magnetic field is governed by the following equations which express the conservation of mass and momentum,

$$\frac{\partial V}{\partial t} + (V.\nabla)V = -\nabla p + \frac{1}{\mathrm{Re}}\Delta V + N(j \times B), \qquad (1)$$

$$\nabla \cdot V = 0 \qquad (2)$$

together with the induced magnetic field equation and the conservation for the magnetic field under the classical MHD assumptions[6,7],

$$\frac{\partial B}{\partial t} - \nabla \times (V \times B) + \nabla \times (\frac{1}{\sigma \mu_m} \nabla \times B) = 0 \qquad (3)$$

$$\nabla \cdot B = 0 \qquad (4)$$

where the magnetic field B includes both the applied (B_o) and induced (B') fields. Here, it should be pointed out that the magnetic free-divergence constraint (4) is implicit in Eq. (3). Indeed, if the divergence of Eq. (3) is taken term by term, the following condition on the divergence of B is obtained:

$$\frac{\partial (\nabla \cdot B)}{\partial t} = 0 \qquad (5)$$

Eq.(5) implies that the divergence of B remains constant over time and thus zero if it is initially null.

Solving the induction (Eq. 3) and the continuity (Eq. 4) equations for the magnetic field would normally result in an over-specified system of equations. This problem can be overcome by applying the continuity equation into the induction equation, while deriving a diffusion-convection Helmholtz-like equation,

$$\frac{\partial B}{\partial t} + (V \cdot \nabla) B = \frac{1}{\sigma \mu_m} \nabla^2 B + (B \cdot \nabla) V , \qquad (6)$$

hence reducing the MHD system of Eqs. (3) and (4) to Eq. (6) with the appropriate set of boundary conditions (here, a constant electric conductivity is assumed locally). It should be noted that circumventing the constraint (4) by solving Eq. (6) results in a much simpler system to solve. However, Eq. (6) no longer states that the divergence of B remains constant over time. To resolve this issue, a penalty factor is introduced to force the magnetic divergence toward zero

based on the technique discussed in References [5,6,8]. The technique calls for an addition of the gradient of a scalar variable q to Eq. (7), which results in the following equation:

$$\frac{\partial B}{\partial t} + (V \cdot \nabla)B = \frac{1}{\sigma \mu_m} \nabla^2 B + (B \cdot \nabla)V + \nabla q \qquad (7)$$

where $q = 0$ on the boundary, q can be viewed as a Lagrange multiplier used to enforce the divergence-free condition.

Once Eqs. (7) and (4) are solved for the induced magnetic field, the induced current can be deduced from the following equation:

$$j = \frac{1}{\mu_m} \nabla \times B \qquad (8)$$

1.1 Free Surface Treatment

The calculation domain involves free surfaces, thus a numerical technique is required to capture its evolution. The Volume of Fluid (VOF) method is incorporated into FLOW3D for this purpose since it is a robust, powerful, extensively applied technique. Two steps are required to complete tracking of the free surface. First, a VOF advection algorithm is required to determine the volume fraction data at the new time step from the old velocity field and the interface location; second, an interface reconstruction algorithm is needed to determine an interface from the given fraction data. A detailed description of this technique can be found in [4, 9-10]. In our one fluid problem, fluid exists where F=1, and void regions correspond to the locations where F=0 and $0 < F < 1$ denotes a free surface cell.

The electric conductivity at any free surface calculation cell varies according to the fraction of the fluid existing in the cell. The electric conductivity is estimated as:

$$\sigma_e = F * \sigma_f + (1 - F) * \sigma_v \qquad (9)$$

where, σ_f and σ_v are the electric conductivity of fluid and void, respectively, and F is a function, which represents a volume fractional amount of fluid in the cell estimated based on the VOF free surface tracking technique. The electric conductivity for the fluid/solid boundary cell is estimated in the same manner as Eq. 9.

1.2 Boundary conditions setting

Due to its 3D nature, the mathematics formulation for induced magnetic boundary conditions at the interface can be very complex. At present we do not know the precise boundaries. However, as discussed by N. B. Salah[5] and L. Leboucher[11], since the permeability is constant, the magnetic field at the boundaries between the two domains is continuous and therefore no boundary conditions need to be specified. Furthermore, we expect that the magnetic field attenuates and vanishes at some distance in the insulating material because of the lack of a source of field generation. A separate study is performed to estimate the "null" distance for a given field strength at the very front by setting velocity equal to zero in equation 7 while satisfying divergent B equal to zero. The calculation indicates that this distance is relatively short (< 1 cm) for the field strength encountered in the present study (< tenth of T). Based on this, the probable boundary conditions are derived at the outside boundary:

$$n \cdot B = 0 \qquad \text{on } \Gamma_1 \qquad (10)$$

$$n \times B = 0 \qquad \text{on } \Gamma_2 \qquad (11)$$

To ensure that the boundary conditions (10) (11) are correct, we use a thick insulating wall as the second domain (which surrounds the flow domain) to allow for the induced magnetic field to drop to zero at its outside boundary.

2. Numerical Schemes

The numerical scheme discussed here relates to the scheme to solve the induced magnetic field equation (7). Numerical methods for solving the Navier-Stoke equations are well documented elsewhere [4, 10]. Numerically, the induction equation is discretized according to the central difference scheme, in which the induced magnetic field is specified at the cell center. The resulting set of algebraic equations are then solved iteratively using the Gause-Siedel technique applying boundary conditions (10-11) at each time step. To achieve a stable numerical solution throughout the simulation, the time step Δt has to satisfy the following criterion:

$$\Delta t \le \frac{\sigma \mu_m}{2(\Delta x^{-2} + \Delta y^{-2} + \Delta z^{-2})} \qquad (12)$$

where Δx, Δy, and Δz are the calculation grid sizes in a Cartesian coordinate system. According to L.Lebourcher[11], this time step

$$\Delta t \le \frac{\mathrm{Re}}{2(\Delta x^{-2} + \Delta y^{-2} + \Delta z^{-2}) + \mathrm{Re}\, N} \qquad (13)$$

is much smaller than that of Eq. 12. Such a stringent time step requirement results in an extremely long CPU time (3-4 weeks) in a 2 GHz PC processor to complete a free surface film flow run, as presented in this paper. At present, results can only be obtained for cases with $\frac{\partial B}{\partial t} = 0$.

3. Results and Discussion

The NSTX outboard midplane 3D magnetic field strengths are shown in Fig.1. Here, the radial field varies along the flow direction (x-coordinate) and forms a transverse field gradient with respect to the flow. The calculated results of the lithium fluid flow along the NSTX

outboard midplane proceeding from a uniform, inlet of 10m/s and an initial film thickness of 2 mm is shown in Figure 2. As shown, much of the solid substrate has been left bare due to the fluid being pushed and spilling over one side of the chute. This feature of spilling over one side of the chute is the result of the poloidal (x direction) return current induced by the surface normal field gradient interacting with the toroidal field and can not be shown with a 2D model.

Another feature of the flow is the development of a M-shape velocity profile, which can be seen near the entrance where the pushing force is not yet strong enough to divert the flow. This can be seen in Figure 3, which shows the evolution of the main velocity (U) component at xy plane of z=7mm. The formation of the M-shape velocity is a consequence of the interaction between the u velocity gradient and the applied magnetic field, which generates the induced magnetic field in the poloidal direction and consequently of the induced currents in toroidal and radial components (j_y and j_z, respectively). The impact on the flow is a Lorentz force opposing fluid flow in the core to cause the fluid to decelerate, while accelerating the fluid flow in both Hartmann and Hunt layers. The contours of B'_x at the yz plane for x=4cm and of B'z at xy plane are shown in Fig.4 (a) and Fig. 4(b). Note that the B'_x is constructed by many loops that close at the wall boundary layer thereby implying a large u velocity gradient.

Furthermore, the interaction between the surface normal field gradient and the main velocity component results in the induced magnetic field in the radial direction. The induced magnetic field in the radial axis is non-symmetric, its variation along the toroidal direction is the cause for the generation of the induced poloidal current. Fig. 5 shows the poloidal currents j_x distribution at yz plane due to the surface normal field gradient. The non-symmetric nature of this current j_x results in non-uniform toroidal Lorenz forces ($F_y = -j_x B_z$) at the two Hunt layer sides. The net integral effect is a toroidal force pushing fluid toward one side.

The problem related to the aforementioned calculated flow behavior is the protection of the exposed solid surface with respect to the surface heat fluxes. In order to overcome the phenomena in which the fluid is pushed to one side, leaving a bare zone, the center axis of the chute is titled 30 degrees away from the surface normal plane. This allows the flow to closely align with the field line, and reduces the magnitude and its effect of the surface normal field observed by the fluid. As a result (as shown in Figures 5 and 6), the undesired feature associated with the spanwise Lorentz force is eliminated, while no bare spot remains in this modified design. The low velocity magnitudes observed at the downstream can be resolved by increasing the inlet velocity (a velocity of 10 m/s is desired from the surface heat flux removal point of view).

4. Conclusions

This paper has presented a new numerical method based on the induced-magnetic-fields equation that can be applied to a 3D free surface flow in a strong magnetic field. From our results, we conclude the following:

The method achieves good convergence of 3D free surface MHD flow at a Hartmann number of 451 by assuming that the induced magnetic field equals zero at the outside boundaries of a thick insulated wall. The magnetic field is assumed continuously at the wall and fluid interface. The next step is to benchmark experimental results that are to be obtained from the MTOR facility.

The 3D MHD effects considered here result in most of the fluid spilling over one side of the chute due to the gradient of surface normal magnetic fields. The reason is that the normal magnetic field gradient leads to poloidally return currents, which interact with the surface normal

field to cause a substantial transverse Lorentz force. These phenomena can not be shown by a 2D model.

Through the modification of the chute axis with respect to the gravity direction, the MHD effect of a surface normal field gradient can be reduced. The results show that the adverse feature of fluid being pushed to one side can be remedied if the chute is tilted 30 degrees off the axis along the toroidal direction.

Acknowledgement

The authors would like to thank Drs. S. Smolentsev and N.B. Morley for helpful discussions and Mike Kotschenreuther for insightful inputs. This work is supported by the U.S. Department of Energy under Grand No. DE-FG03-86ER52123.

References

[1] M. Kotschenreuther, The effects of surface normal magnetic fields on concepts for fast surface flows of liquid metals, including toroidal breaks. APEX Memorandum, March 16, 2001.

[2] J. S. Walker, et.al., Three-dimensional MHD duct flows with strong transverse magnetic fields. Part 3. Variable-area rectangular ducts with insulating walls, J.Fluid Mech. **56**, (1972) 121.

[3] A. Potherat, et.al, An Effective Two-Dimensional Model for MHD Flows with Transverse Magnetic Field, J.Fluid Mech, **424**, (2000) 75.

[4] FLOW-3D User's Manual, Version 7.7, Flow Science Inc., 2000.

[5] N. B. Salah, A. Soulaimani, and W. G. Habashi, A finite element method for magnetohydrodynamics, Comput. Methods Appl. Mech. Engrg. 190(2001) 5867-5892.

[6] L. D. Landau, E. M. Lifshitz, L. P. Pitaevskii, Electrodynamics of Continuous Media, Pergamon Press, Oxford, 1984.

[7] H. Branover, Magnetohydrodynamic Flow in Ducts, Israel University Press, Jerusalem, Israel, 1978.

[8] B. Jiang, J.Wu, L.A.Povinelli, The origin of spurious solutions in computational electromagnetics, NASA-TM-106921, E-9633, ICOMP-95-8, 1995.

[9] C. W. Hirt and B. D. Nichols, Volume of Fluid (VOF) Method for the Dynamics of Free Boundaries, J.Comp. Phys., **39**, (1981) 201.

[10] E. G. Puckett, A. S. Almgren, J. B. Bell, et al., "A high-order projection method for tracking fluid interfaces in variable density incompressible flow", J Journal of Computational Physics, 130 (1997) 269-282.

[11] L. Leboucher, Monotone Scheme and Boundary Conditions for Finite Volume Simulation of Magnetohydrohynamic Internal Flow at High hartmann Number, Journal of Computational Physics, 150(1999) 181-198.

Nomenclature

B Magnetic field vector (T);

F Volume function of fluid;

j current density (vector);

N= $\frac{\sigma B_0^2 L}{\rho U}$ Interaction Parameter;

n normal vector;

Greece:

σ electric conductivity;

μ magnetic permeability;

Δt time step (s);

Δx x direction grid size of cell;

p Pressure (N/m^2);

q scalar variable;

Re=UL/ν Reynolds Number;

t time (s);

V Velocity Vector;

Δy y direction grid size of cell;

Δz z direction grid size of cell;

Subscript:

e effective;

m magnetic field;

v void(wall).

FIGURE CAPTIONS

Figure 1. NSTX outboard midplane 3D magnetic fields versus x. (x denotes poloidal direction, y: toroidal and z : radial)

Figure 2. 3D free surface MHD fluid flow at the midplane of NSTX. Contours are u velocity variables.

Figure 3. U velocity profile at XY plane of z=7mm.

Figure 4. Induced magnetic field B'_x contour at YZ plane of x=4cm (a) and induced magnetic field B'_z contour at XY plane of Z=7mm (b).

Figure 5. Induced current j_x contour at YZ plane of x=4cm.

Figure 6. 3D free surface MHD fluid flow at the modified chute of NSTX midplane. Contours are u velocity variables.

Figure 7. U velocity profile at XY plane of z=7mm.

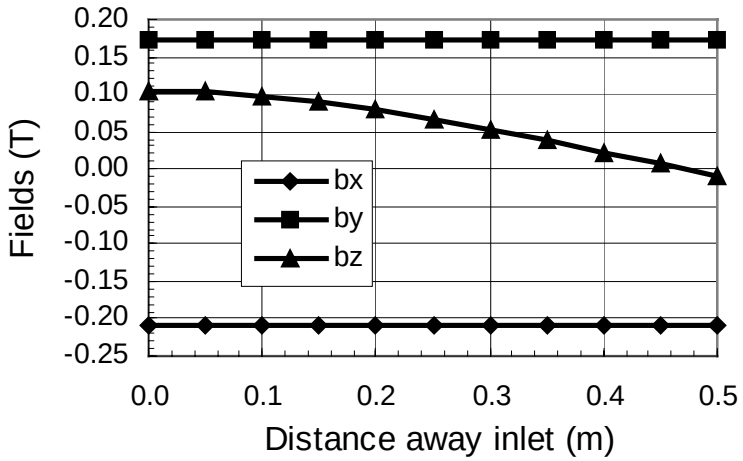

Fig.1. NSTX outboard midplane 3D magnetic fields versus x.
(x denotes poloidal direction, y: toroidal and z : radial)

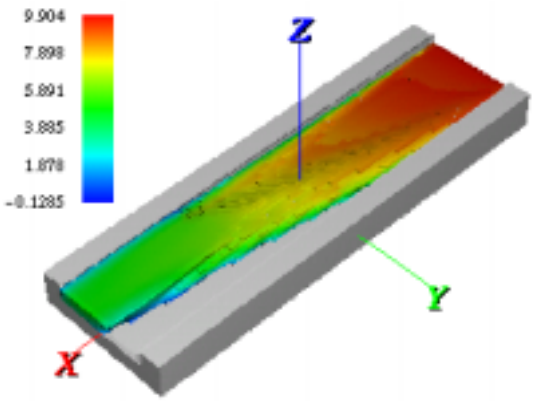

Fig. 2. 3D free surface MHD fluid flow at the midplane of NSTX. Contours are u velocity variables.

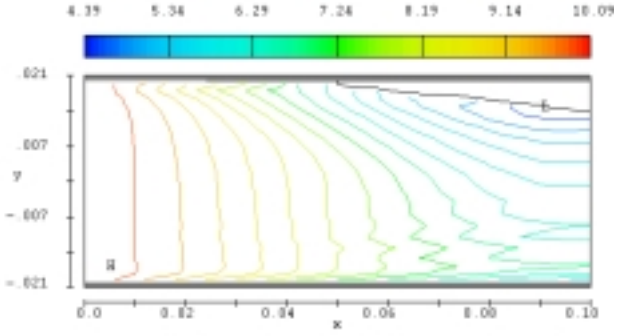

Fig.3. U velocity profile at XY plane of z=7mm.

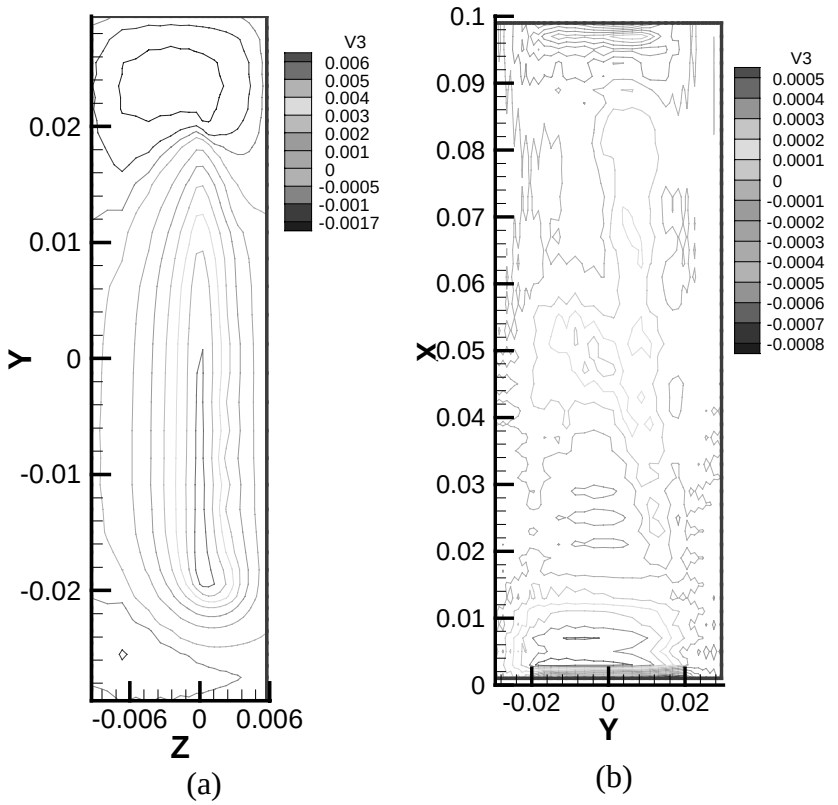

Fig. 4. Induced magnetic field B'_x contour at YZ palne of x=4cm (a) and induced magnetic field B'_z contour at XY palne of Z=7mm (b).

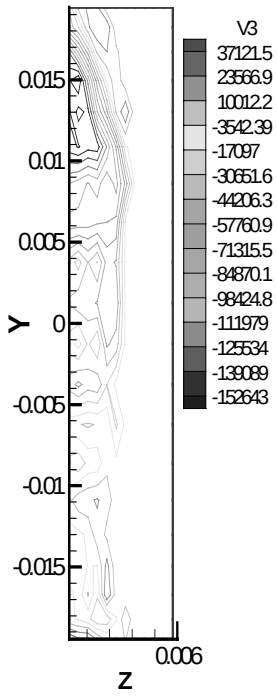

Fig. 5. Induced current j_x contour at YZ palne of x=4cm.

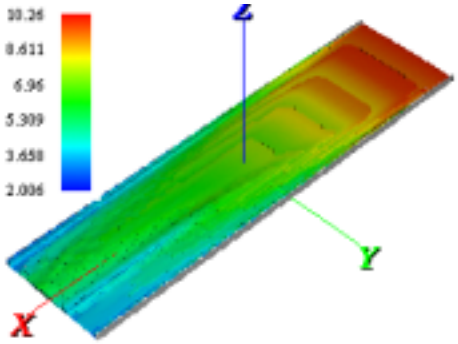

Fig.6. 3D free surface MHD fluid flow at the modified chute of NSTX midplane. Contours are u velocity variables.

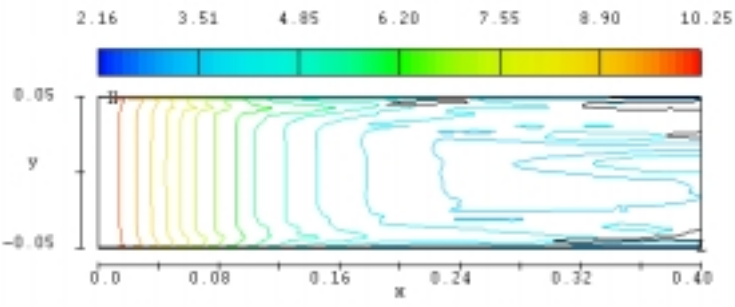

Fig.7. U velocity profile at XY plane of z=7mm.